

Robust Control For Spacecraft Attitude Tracking Under Multiple Physical Limitations with Guaranteed Performance

Jiakun Lei, Tao Meng, Weijia Wang, Chengjin Yin, Zhonghe Jin

Abstract—This paper considers the prescribed performance control (PPC) of spacecraft attitude tracking under multiple physical constraints, focusing on the robust issues. A novel Barrier Lyapunov function is proposed to realize the guaranteed-performance control under angular velocity constraint without singularity. Additionally, an adaptive strategy for the performance function is presented to soften the constraint and quickly re-stabilize the system after severe disturbances occur, providing strong robustness. Further, an auxiliary system is designed to handle the input saturation issue, incorporating the actuator limitation into the system. Based on the proposed structure, a backstepping controller is developed accordingly using a double-layer PPC framework. Numerical simulation results are presented to validate the proposed controller framework's efficiency and robustness.

Index Terms—Attitude Tracking Control , Prescribed Performance Control , Physical Constraints , Barrier Lyapunov Function

I. INTRODUCTION

For a real aerospace engineering space mission, constraints, performance, and robustness are eternal topics, such as the physical limitation including angular velocity constraint and torque output limitation. Besides, some performance requirements, including maximum settling time and steady-state control accuracy, are required to be satisfying, while the robustness of a system should be guaranteed. Generally speaking, these requirements may be hard to satisfy simultaneously. Motivated by this issue, this paper investigates the possible way to satisfy all these requirements in attitude tracking problems while ensuring the system appears strong robustness for severe perturbation.

Many works related to this field have been discovered before. As for the attitude control problem under angular velocity constraint, it has been widely discovered by many researchers due to its application value. In [1], a quaternion-based feedback control law is proposed with the consideration of angular rate limitation and torque limitation. Nevertheless,

the proposed controller lacks strict proof of its stability. Based on the idea of potential field, [2] presents a nonlinear controller to deal with the angular velocity constraint and the control saturation issue. In [3], by utilizing the backstepping methodology, the virtual control law is designed to be explicitly bounded using the hyperbolic tangent function, and the angular velocity limitation is tackled in this way. Similarly, the actuator output limitation is one of the most widely discussed constraints for the attitude control problem. Generally speaking, this issue is usually solved by introducing the auxiliary system, as introduced in [4]–[6].

The attitude control problem with preassigned performance requirements has been of high-interest in recent years, and the prescribed performance control (PPC) scheme is often adopted to handle this problem, as stated in [7]–[10]. However, the traditional PPC scheme has the inherent risk of suffering from the singularity problem. As elaborated in [11], a premise should be guaranteed for PPC such that the state constraint should stay in the constraint region at any time. Nevertheless, although this premise can be guaranteed technically at the initial condition, this premise may still not be able to satisfy when there exists significant external disturbance or input saturation [12], [13]. This inherent problem significantly lowers the application value of traditional PPC in real engineering scenarios, and this issue has recently raised some attention, with several efficient solutions proposed. In [12], [14], we propose two solutions individually, whose main idea is to loosen the original hard constraint into a soft one, ensuring that the PPC framework can work appropriately even when the constraint is violated. In [13], an auxiliary feedback system for the performance function is proposed to generate an additional signal, ensuring that the performance function's envelope can cover the state trajectory under any condition, and the singularity is circumvented in this way.

According to the existing work, for an efficient scheme fusing all these requirements, there is still a lack up to now. Although the PPC control under physical limitation has been investigated in [15] recently and has provided a motivated solution, it still failed to handle the critical singularity problem. In this paper, we are dedicated to satisfying all these constraints simultaneously. Compared with existing works, this paper delivers a possible framework to fuse the physical limitation, performance requirements, and robust characteristics together. The main contribution of this paper can be summarized as follows:

1. A newly-designed Barrier Lyapunov function is pro-

Jiakun Lei, Ph.D., School of Aeronautics and Astronautics, Zhejiang University, Hangzhou, China, 310027, 12124010@zju.edu.cn

Tao Meng, Prof., School of Aeronautics and Astronautics, Zhejiang University, Hangzhou, China, 310027, mengtao@zju.edu.cn

Weijia Wang, Ph.D., School of Aeronautics and Astronautics, Zhejiang University, Hangzhou, China, 310027, 12024055@zju.edu.cn

Chengjin Yin, M.S., School of Aeronautics and Astronautics, Zhejiang University, Hangzhou, China, 310027, 22124030@zju.edu.cn

Zhonghe Jin, Prof., School of Aeronautics and Astronautics, Zhejiang University, Hangzhou, China, 310027, Zhejiang Key Laboratory of micro-nano-satellite, jinzh@zju.edu.cn

posed to cope with the attitude tracking with preassigned performance requirements under angular velocity constraints. Further, the singularity problem is circumvented simultaneously. **2.** An adaptive strategy for performance function is designed, ensuring that the system is able to re-stabilize short after a sudden severe disturbance occurs, providing strong robustness for the system. **3.** Due to the consideration of many constraints and the singularity problem, the proposed scheme may be of higher application value compared with traditional PPC schemes.

The rest of this paper is organized as follows: the problem formulation and mathematical lemma introduction are delivered in section II separately, while the main idea of the proposed solution is elaborated in section IV. Controller derivation is proposed in V, and the final simulation validation of the proposed scheme is detailed in section VI.

II. PROBLEM FORMULATION

A. Notations

Following notations are defined for this paper. \mathbf{I}_n represents the $n \times n$ identity matrix, while $\|\cdot\|$ denotes the Euclidean norm of a vector or the induced norm of a matrix. The operator symbol \mathbf{b}^\times denotes the 3×3 skew-symmetric matrix for vector cross manipulation, i.e. $\mathbf{b}^\times \mathbf{s} = \mathbf{b} \times \mathbf{s}$. Further, $\text{diag}(b_i)$ represents a diagonal matrix whose diagonal line is consisted by the components of the given vector \mathbf{b} , and $\text{vec}(b_i)$ denotes a column vector such that $\text{vec}(b_i) = [b_1, b_2, \dots, b_i]^\top$.

B. Attitude System Modeling

Considering the attitude error system of a rigid-body spacecraft, its kinematic and dynamic system expressed in the normalized attitude error quaternion is expressed as follows [16]:

$$\begin{aligned} \dot{\mathbf{q}}_{ev} &= \mathbf{F}_e \boldsymbol{\omega}_e & \dot{q}_{e0} &= -\frac{1}{2} \mathbf{q}_{ev}^\top \boldsymbol{\omega}_e \\ \mathbf{J} \dot{\boldsymbol{\omega}}_e &= \mathbf{M}_0 + \boldsymbol{\tau} + \mathbf{d} \end{aligned} \quad (1)$$

where the attitude error quaternion is denoted as $\mathbf{q}_e = [\mathbf{q}_{ev}^\top, q_{e0}]^\top \in \mathbb{R}^4$. The vector part and the scalar part of the attitude error quaternion is expressed as \mathbf{q}_{ev} and q_{e0} , receptively. The inertial matrix of the spacecraft expressed in the body-fixed frame is denoted as $\mathbf{J} \in \mathbb{R}^{3 \times 3}$, where \mathbf{J} is a symmetric positive-definite matrix all along. $\boldsymbol{\tau} \in \mathbb{R}^3$ represents the system's control input, while $\mathbf{d} \in \mathbb{R}^3$ denotes the lumped unknown external disturbances. Denote the desired angular velocity expressed in the desired body-fixed frame \mathfrak{R}_d as $\boldsymbol{\omega}_d$, the error angular velocity expressed in the current body-fixed frame can be expressed as $\boldsymbol{\omega}_e = \boldsymbol{\omega}_s - \mathbf{C}_e \boldsymbol{\omega}_d$, where $\boldsymbol{\omega}_s$ represents the current body-fixed angular velocity with respect to the inertial frame, and \mathbf{C}_e denotes the transformation matrix from \mathfrak{R}_d to \mathfrak{R}_b . $\mathbf{M}_0 = \mathbf{J} \boldsymbol{\omega}_e^\times \mathbf{C}_e \boldsymbol{\omega}_d - \mathbf{J} \mathbf{C}_e \dot{\boldsymbol{\omega}}_d - \boldsymbol{\omega}_s^\times \mathbf{J} \boldsymbol{\omega}_s$ represents the lumped dynamical term, \mathbf{F}_e represents the Jacobian matrix of attitude error kinematic expressed as $\mathbf{F}_e = \frac{1}{2} (q_{e0} \mathbf{I}_3 + \mathbf{q}_{ev}^\times)$. Note that the following property will be hold such that $\|\mathbf{F}_e^{-1}\| = \frac{2}{|q_{e0}|}$.

For the following analysis, define a saturation variable as $\Delta \boldsymbol{\tau} = \boldsymbol{\tau} - \mathbf{u}$, where \mathbf{u} represents the command control input derived by controller.

C. Assumptions

For the synthesize of the proposed control scheme, these assumptions are made in this paper.

Assumption 1. The inertial matrix \mathbf{J} of the spacecraft is a known symmetric positive-definite matrix. Accordingly, we have:

$$\lambda(\mathbf{J})_{\min} \mathbf{x}^\top \mathbf{x} \leq \mathbf{x}^\top \mathbf{J} \mathbf{x} \leq \lambda(\mathbf{J})_{\max} \mathbf{x}^\top \mathbf{x} \quad (2)$$

where $\lambda(\cdot)$ represents the corresponding eigen value.

Assumption 2. The external disturbance is unknown but bounded by a known constant, i.e., $\|\mathbf{d}\| \leq D_m$.

III. CONTROL OBJECTIVE

The primary purpose of this paper is to develop a relevant controller to ensure that the given physical constraints and performance requirements can be satisfied simultaneously. Also, the ultimate boundedness of the closed-loop signals should be guaranteed. Further, another purpose of this paper is to ensure that the system can rapidly recover from significant sudden external disturbances.

IV. PROBLEM SOLUTION

A. Error Transformation Procedure

As stated in [17], the performance function should be assigned according to the given performance requirements firstly. Defining a performance function vector as $\boldsymbol{\rho}(t) = [\rho_1(t), \dots, \rho_i(t)]^\top \in \mathbb{R}^3$ ($i = 1, 2, 3$), considering arbitrary system state variable denoted as $\mathbf{e}(t) = [e_1(t), \dots, e_i(t)]^\top \in \mathbb{R}^3$, the state constraint for $e_i(t)$ can be expressed as follows:

$$-\rho_i(t) < e_i(t) < \rho_i(t) \quad (3)$$

Further, defining a translated error variable corresponding to $\mathbf{e}(t)$ as $\boldsymbol{\varepsilon}(t) = [\varepsilon_1(t), \dots, \varepsilon_i(t)]^\top \in \mathbb{R}^3$ ($i = 1, 2, 3$), and the i th component of $\boldsymbol{\varepsilon}$ is defined as $\varepsilon_i(t) = \frac{e_i(t)}{\rho_i(t)}$. Accordingly, the expected state constraint 3 can be transformed into an equivalently one expressed as $|\varepsilon_i(t)| < 1$. Since $|\varepsilon_i| < 1$ will be hold if $\|\boldsymbol{\varepsilon}\|^2 < 1$ is satisfied, thus we strengthen the original constraint into the stronger one.

B. Barrier Lyapunov Function Design

Inspired by our previous work [14], to realize a non-singular PPC control under angular velocity limitations, we propose the following Barrier Lyapunov Function V_B in this paper:

$$V_B = \frac{k}{2} F \ln [\cosh(\boldsymbol{\varepsilon}^\top \boldsymbol{\varepsilon} / F)] \quad (4)$$

where $k > 0$ and $F > 0$ are the design parameters. Take the the gradient of the proposed BLF V_B with respect to $\boldsymbol{\varepsilon}$, we have:

$$\nabla_{\boldsymbol{\varepsilon}} V_B = k \tanh(\boldsymbol{\varepsilon}^\top \boldsymbol{\varepsilon} / F) \boldsymbol{\varepsilon}^\top \quad (5)$$

Compared with the mostly-applied logarithmic-type BLF expressed as $V_i = \frac{1}{2} \ln \left(\frac{1}{1 - \|\boldsymbol{\varepsilon}\|^2} \right)$, notably, $\|\nabla_{\boldsymbol{\varepsilon}} V_i\| \rightarrow \infty$ will be hold if $\|\boldsymbol{\varepsilon}\|^2 \rightarrow 1$ is hold, while $\|\nabla_{\boldsymbol{\varepsilon}} V_B\|$ will not tend to infinity under such a condition. Therefore, the gradient of the proposed BLF will increasing at a relatively slow rate when

$\|\varepsilon\|^2 \rightarrow 1$, providing mild controller output. Applying the proposed BLF will turn the original "hard" constraint into a soft one. However, the asymptotical convergence of ε is still guaranteed. For the following analysis, considering a function $v(x) = \ln(\cosh(x))$ ($x \geq 0$), these following properties will be obtained.

Property 1. $\frac{1}{2}x \tanh(x) \leq \ln[\cosh(x)] \leq x \tanh(x)$ will be hold for $\forall x \in [0, +\infty)$.

Define $g(x) = \ln[\cosh(x)] - \frac{1}{2}x \tanh(x)$, considering $\cosh(x) \cdot \dot{g}(x)$, the property will be easily obtained.

Property 2. For $k > 0$, there exists a constant m , $k_0 < k$ such that $k \tanh(mx) \geq x$ will be satisfied on $x \in [0, +k_0)$ all along.

This property can be proved geometrically easily, here we omitted for brevity.

C. Prescribed Performance Function Design

In this paper, the prescribed performance function (PPF) is designed to be a composite one, consisting of a nominal part and an adaptive-updated part.

1. Nominal Part of PPF

The nominal part of the PPF is designed the same as the one stated in [12], expressed as follows:

$$\rho_n(t) = \begin{cases} \rho_e(t) = (\rho_{e0} - \rho_{e\infty})e^{-lt} + \rho_{e\infty} & 0 \leq t < t_1 \\ \rho_p(t) = a_1 t^2 + a_2 t + a_3 & t_1 \leq t < t_2 \\ \rho_c(t) = g_\infty & t_2 \leq t \end{cases} \quad (6)$$

where $t_2 > 0$ stands for the preassigned settling time, ρ_{e0} , $\rho_{e\infty}$ denotes the initial value and the terminal value of the the exponential function part respectively, g_∞ denotes the terminal value. a_1 , a_2 , a_3 and t_1 are coefficients needs solving later, where t_1 represents the time instant such that $\rho_e(t_1) = \rho_p(t_1)$ is satisfied. By indicating t_2 , ρ_{e0} , $\rho_{e\infty}$, g_∞ and l , the coefficient t_1 , a_1 , a_2 , a_3 can be calculated according to the smoothness connection condition, expressed as follows:

$$\begin{cases} \left[\frac{k}{2}(t_2 - t_1) - 1 \right] (\rho_{e0} - \rho_{e\infty})e^{-lt_1} - \rho_{e\infty} + g_\infty = 0 \\ a_1 = (\rho_{e0} - \rho_{e\infty})e^{-lt_1} / 2(t_1 - t_2) \\ a_2 = -2a_1 t_2 \\ a_3 = g_\infty + a_1 t_2^2 \end{cases} \quad (7)$$

Note that the selecting of the parameter should guarantee that a real-number solution exists for the equation (7).

Remark 1. One main characteristic of the introduced PPF is that by choosing appropriate parameters, t_1 can be set close enough to t_2 such that $t_1 - t_2 \rightarrow 0$, which vanishes the parabola curve part practically. This property will make sense in the following controller design section.

2. Adaptive Performance Function Strategy

In order to alleviate the over-control problem when the system suffers from strong disturbances, an adaptive strategy for the performance function is proposed. Denote the adaptive

part of PPF as $\Delta\rho$. The adaptive strategy takes the following form:

$$\Delta\dot{\rho} = -K_\rho \Delta\rho + K_\tau \text{vec}(|\tanh c_\tau \Delta\tau_i|) \quad (8)$$

where K_ρ , K_τ , c_τ are design parameters that needs indicating. The primary mechanism of the proposed adaptive strategy for PPF can be elaborated as follows: When the input saturation happens, $\Delta\rho$ will be triggered by $|\tanh c_\tau \Delta\tau_i|$. Thus, it generates a bounded positive signal to ρ_i . This will establish a wider constraint boundary, significantly reducing the value of ε . Therefore, the over-control problem will be alleviated in this way.

Assume that the state trajectory is disturbed by external disturbances at a steady state, then the state trajectory will deviate from the original status. Notably, since ρ_i has converged to a small value, thus ε_i will have several orders of magnitude increasing, and $\varepsilon_i = e_i/\rho_i$ will be a big value under such a condition. This will produce a tremendous control input for the system, causing intensive chattering of the state trajectory. This problem will be validated later in section VI.

Remark 2. Different from the work in [13], since the newly-designed BLF solves the singularity problem, the primary purpose of introducing the adaptive strategy for PPF is to alleviate the chattering and smooth the system's convergence behavior. Hence, it derives a simple adaptive law, and the state variable is unnecessarily fed to our scheme's adaptive strategy.

By combining the nominal part ρ_n and the adaptive part $\Delta\rho$ of the PPF, the composite PPF ρ is defined as $\rho = \rho_n + \Delta\rho$

V. CONTROL LAW DERIVATION

Based on the proposed BLF, a backstepping controller is developed using a double-layered PPC structure. Simultaneously, an adaptive strategy of PPF and an auxiliary system are designed to cope with the over-control and input saturation issues respectively. The sketch map of the proposed controller is illustrated as in Figure 1:

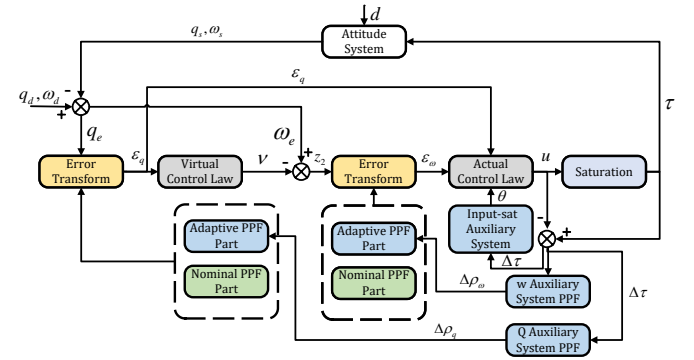


Fig. 1: System Diagram

Define the PPF of q_{ev} as $\rho_q = \rho_{q0} + \Delta\rho_q$, where ρ_{q0} and $\Delta\rho_q$ denote the nominal part and the adaptive part correspondingly. Let ρ_{qi} denotes the i th component of the PPF for following analysis. Define the corresponding transformed

error variable of \mathbf{q}_{ev} as $\boldsymbol{\varepsilon}_q = [\varepsilon_{q1}, \dots, \varepsilon_{qi}]^T \in \mathbb{R}^3$ such that $\varepsilon_{qi} = q_{evi}/\rho_{qi}$ is hold. For further analyzing, considering the following two subsystem $\mathbf{z}_1, \mathbf{z}_2$ as:

$$\mathbf{z}_1 = \boldsymbol{\varepsilon}_q \quad \mathbf{z}_2 = \boldsymbol{\omega}_e - \mathbf{v} \quad (9)$$

where \mathbf{v} denotes the virtual control law of \mathbf{z}_1 layer.

Step 1. In view of the typical backstepping methodology, regard the attitude error angular velocity $\boldsymbol{\omega}_e$ as the virtual control law \mathbf{v} . Take the time-derivative of \mathbf{z}_1 , one has:

$$\dot{\mathbf{z}}_1 = \dot{\boldsymbol{\varepsilon}}_q = \boldsymbol{\psi}_q \mathbf{F}_e \boldsymbol{\omega}_e - \boldsymbol{\psi}_q \boldsymbol{\eta}_q \mathbf{q}_{ev} \quad (10)$$

where $\boldsymbol{\psi}_q = \text{diag}(\psi_{q1}, \dots, \psi_{qi}) \in \mathbb{R}^{3 \times 3}$ ($i = 1, 2, 3$) and $\boldsymbol{\eta}_q = \text{diag}(\eta_{q1}, \dots, \eta_{qi}) \in \mathbb{R}^{3 \times 3}$ are diagonal matrices. ψ_{qi} and η_{qi} are defined as follows:

$$\psi_{qi} = 1/\rho_{qi}; \quad \eta_{qi} = \dot{\rho}_{qi}/\rho_{qi} \quad (11)$$

Applying these notations, the virtual control law \mathbf{v} is designed and expressed as follows:

$$\mathbf{v} = -\frac{|q_{e0}|}{2} k M_\omega \mathbf{F}_e^{-1} \boldsymbol{\psi}_q^{-1} \text{vec}(\tanh \beta \boldsymbol{\varepsilon}_{qi}) \quad (12)$$

where $M_\omega > 0$ is a design parameter, $\beta > 0$ is a big enough coefficient needs indicating, $k > 1$ is a design parameter, $\text{vec}(\tanh \beta \boldsymbol{\varepsilon}_{qi})$ denotes the \mathbb{R}^3 element-spanned column vector.

Remark 3. note $\|\mathbf{F}_e^{-1}\| = \frac{2}{|q_{e0}|}$, therefore the norm of the virtual control law satisfies: $\|\mathbf{v}\| \leq k M_\omega \frac{|q_{e0}|}{2} \|\mathbf{F}_e^{-1}\| \|\boldsymbol{\psi}_q^{-1}\| \leq k M_\omega (\|\rho_{qi}\|)_{\max}$. Owing to the fact that $|\rho_{qi}| < 1$, it derives that $\|\mathbf{v}\| < k M_\omega$ will be always hold.

Based on the proposed BLF, a candidate Lyapunov function V_1 is selected as follows:

$$V_1 = \frac{1}{2} k_1 F_1 \ln [\cosh (\boldsymbol{\varepsilon}_q^T \boldsymbol{\varepsilon}_q / F_1)] \quad (13)$$

where k_1, F_1 are positive design parameters. Take the time-derivative of V_1 , one has:

$$\dot{V}_1 = k_1 \tanh (\boldsymbol{\varepsilon}_q^T \boldsymbol{\varepsilon}_q / F_1) \boldsymbol{\varepsilon}_q^T [\boldsymbol{\psi}_q \mathbf{F}_e \boldsymbol{\omega}_e - \boldsymbol{\psi}_q \boldsymbol{\eta}_q \mathbf{q}_{ev}] \quad (14)$$

Substituting the virtual control law (12) into \dot{V}_1 yields:

$$\begin{aligned} \dot{V}_1 = & -\frac{|q_{e0}| k M_\omega}{2} k_1 \tanh (\boldsymbol{\varepsilon}_q^T \boldsymbol{\varepsilon}_q / F_1) \boldsymbol{\varepsilon}_q^T \text{vec}(\tanh \beta \boldsymbol{\varepsilon}_{qi}) \\ & + k_1 \tanh (\boldsymbol{\varepsilon}_q^T \boldsymbol{\varepsilon}_q / F_1) \boldsymbol{\varepsilon}_q^T \boldsymbol{\psi}_q \mathbf{F}_e \mathbf{z}_2 \\ & - k_1 \tanh (\boldsymbol{\varepsilon}_q^T \boldsymbol{\varepsilon}_q / F_1) \boldsymbol{\varepsilon}_q^T \boldsymbol{\psi}_q \boldsymbol{\eta}_q \mathbf{q}_{ev} \end{aligned} \quad (15)$$

Hence, according to property 2, by selecting an appropriate k , the first term of (15) can be rearranged into the following form:

$$\begin{aligned} & -\frac{|q_{e0}| k M_\omega}{2} k_1 \tanh (\boldsymbol{\varepsilon}_q^T \boldsymbol{\varepsilon}_q / F_1) \boldsymbol{\varepsilon}_q^T \text{vec}(\tanh \beta \boldsymbol{\varepsilon}_{qi}) \\ & \leq -\frac{|q_{e0}| M_\omega}{2} k_1 \tanh (\boldsymbol{\varepsilon}_q^T \boldsymbol{\varepsilon}_q / F_1) \boldsymbol{\varepsilon}_q^T \boldsymbol{\varepsilon}_q \end{aligned} \quad (16)$$

Remark 4. Considering about the range of $|\varepsilon_{qi}|$. As we elaborated in Subsection IV-B, owing to the designed adaptive system for PPF, the constraint boundary will getting wider if necessary, and this will sharply reduce the value of $|\varepsilon_{qi}|$ under extreme conditions. Therefore, it is rational to say $|\varepsilon_{qi}|$

is practically bounded. In this paper, we set $k = 3$ for the following analysis.

Subsequently, according to the property (1), note that $x \tanh x \geq \ln(\cosh x)$ is hold for $x > 0$. Hence, we have the final result expressed as:

$$-\frac{|q_{e0}| M_\omega}{2} k_1 \tanh (\boldsymbol{\varepsilon}_q^T \boldsymbol{\varepsilon}_q / F_1) \boldsymbol{\varepsilon}_q^T \boldsymbol{\varepsilon}_q \leq -|q_{e0}| M_\omega V_1 \quad (17)$$

Consider the third term in equation (15), owing to the fact that $\varepsilon_{qi} = q_{evi}/\rho_{qi}$, we can notice that $\boldsymbol{\psi}_q \mathbf{q}_{ev} = \boldsymbol{\varepsilon}_q$ will be always hold. Further, according to the property (1), since $\frac{1}{2} x \tanh x \leq \ln \cosh(x)$ is satisfied, thus we have the following result:

$$\begin{aligned} & -k_1 \tanh (\boldsymbol{\varepsilon}_q^T \boldsymbol{\varepsilon}_q / F_1) \boldsymbol{\varepsilon}_q^T \text{diag} \left(\frac{\dot{\rho}_{qi}}{\rho_{qi}} \right) \boldsymbol{\varepsilon}_q \\ & \leq 2 \left(\frac{|\dot{\rho}_{qi}|}{\rho_{qi}} \right)_{\max} \frac{k_1}{2} F_1 \tanh (\boldsymbol{\varepsilon}_q^T \boldsymbol{\varepsilon}_q / F_1) \boldsymbol{\varepsilon}_q^T \boldsymbol{\varepsilon}_q / F_1 \\ & \leq 4 \left(\frac{|\dot{\rho}_{qi}|}{\rho_{qi}} \right)_{\max} \frac{k_1}{2} F_1 \ln [\cosh (\boldsymbol{\varepsilon}_q^T \boldsymbol{\varepsilon}_q / F_1)] \end{aligned} \quad (18)$$

By sort out these results, we have the following conclusion:

$$\begin{aligned} \dot{V}_1 \leq & -\left[|q_{e0}| M_\omega - 4 \left(\frac{|\dot{\rho}_{qi}|}{\rho_{qi}} \right)_{\max} \right] V_1 \\ & + \tanh \left(\frac{\boldsymbol{\varepsilon}_q^T \boldsymbol{\varepsilon}_q}{F_1} \right) \boldsymbol{\varepsilon}_q^T \boldsymbol{\psi}_q \mathbf{F}_e \mathbf{z}_2 \end{aligned} \quad (19)$$

Step 2. Considering the aforementioned error variable $\mathbf{z}_2 = \boldsymbol{\omega}_e - \mathbf{v}$, take the time-derivative of $J\mathbf{z}_2$, one can be obtained that:

$$J\dot{\mathbf{z}}_2 = \mathbf{M}_0 + \mathbf{u} + \mathbf{d} + \Delta\boldsymbol{\tau} - J\dot{\mathbf{v}} \quad (20)$$

where $\mathbf{M}_0 \in \mathbb{R}^3$ denotes the aforementioned dynamical terms, $\Delta\boldsymbol{\tau}$ represents the input saturation stated before. Similarly, the PPF of \mathbf{z}_2 is defined as $\boldsymbol{\rho}_\omega = \boldsymbol{\rho}_{\omega 0} + \Delta\boldsymbol{\rho}_\omega$, where the i th component of $\boldsymbol{\rho}_\omega$ is expressed as $\rho_{\omega i}$. Define the corresponding transformed error variable of \mathbf{z}_2 as $\boldsymbol{\varepsilon}_\omega = [\varepsilon_{\omega 1}, \dots, \varepsilon_{\omega i}]^T \in \mathbb{R}^3$, such that $\varepsilon_\omega = z_{2i}/\rho_{\omega i}$ is hold, therefore the time derivative of $\boldsymbol{\varepsilon}_\omega$ can be expressed as:

$$\dot{\boldsymbol{\varepsilon}}_\omega = \boldsymbol{\xi} \mathbf{J}^{-1} \cdot J\dot{\mathbf{z}}_2 - \boldsymbol{\xi} \boldsymbol{\gamma} \mathbf{z}_2 \quad (21)$$

where $\boldsymbol{\xi}$ is a $\mathbb{R}^{3 \times 3}$ diagonal matrix defined as $\boldsymbol{\xi} = \text{diag}(1/\rho_{\omega i})$ ($i = 1, 2, 3$), $\boldsymbol{\gamma}$ is a $\mathbb{R}^{3 \times 3}$ diagonal matrix defined as $\boldsymbol{\gamma} = \text{diag}(\dot{\rho}_{\omega i}/\rho_{\omega i})$. For the $\boldsymbol{\omega}_e$, the actual command control law \mathbf{u} is designed as follows:

$$\begin{aligned} \mathbf{u} = & -\mathbf{M}_0 - \hat{\mathbf{d}} + J\dot{\mathbf{v}} - K_\omega J\boldsymbol{\xi}^{-1} \boldsymbol{\varepsilon}_\omega + J\boldsymbol{\gamma} \mathbf{z}_2 - K_u J\boldsymbol{\xi}^{-1} \boldsymbol{\theta} \\ & - \frac{\tanh (\boldsymbol{\varepsilon}_q^T \boldsymbol{\varepsilon}_q / F_1)}{k_2 \tanh (\boldsymbol{\varepsilon}_\omega^T \boldsymbol{\varepsilon}_\omega / F_2)} J\boldsymbol{\xi}^{-1} \text{diag}(\rho_{\omega i}) \boldsymbol{\psi}_q \mathbf{F}_e \boldsymbol{\varepsilon}_q \end{aligned} \quad (22)$$

where $\hat{\mathbf{d}} \in \mathbb{R}^3$ denotes the compensation for external disturbance expressed as $\hat{\mathbf{d}} = D_m \text{vec} \left(\tanh \frac{\boldsymbol{\varepsilon}_{\omega i}}{\mu_i} \right)$ ($\mu_i > 0$), K_ω is the controller gain to be designed. An auxiliary system $\boldsymbol{\theta}$ is designed to cope with the drawbacks brought by the input saturation issue, expressed as follows:

$$\dot{\boldsymbol{\theta}} = -\left[K_a + \frac{K_b \|\boldsymbol{\xi} \mathbf{J}^{-1} \Delta\boldsymbol{\tau}\|^2}{\|\boldsymbol{\theta}\|^2} \right] \boldsymbol{\theta} + \boldsymbol{\xi} \mathbf{J}^{-1} \text{vec}(\tanh \Delta\tau_i) \quad (23)$$

where K_a , K_b stands for the gain of the auxiliary system. Specifically, based on the aforementioned idea in subsection IV-C, the adaptive strategy for $\Delta\rho_q$ and $\Delta\rho_\omega$ are designed as follows:

$$\begin{aligned}\Delta\dot{\rho}_q &= -C_q\Delta\rho_q + C_\tau\xi\mathbf{J}^{-1}\text{vec}(|\tanh\Delta\tau_i|) \\ \Delta\dot{\rho}_\omega &= -C_\omega\Delta\rho_\omega + B_\tau\xi\mathbf{J}^{-1}\text{vec}(|\tanh\Delta\tau_i|)\end{aligned}\quad (24)$$

where C_q , C_ω , C_τ , B_τ are gain parameters. By adjusting these parameter, the equilibrium value of the adaptive system is able to be changed arbitrarily. Notably, since the value of $|q_{evi}|$ will never larger than 1, thus the equilibrium value of PPF adaptive strategy should be set accordingly. Choose these candidate Lyapunov functions as follows: $V_2 = \frac{k_2}{2}F_2 \ln[\cosh(\varepsilon_\omega^T\varepsilon_\omega/F_2)]$, $V_3 = \frac{1}{2}\theta^T\theta$, $V_4 = \frac{1}{2}\Delta\rho_q^T\rho_q + \frac{1}{2}\Delta\rho_\omega^T\rho_\omega$. Take the time-derivative of V_2 , one can be obtained that:

$$\dot{V}_2 = k_2 \tanh(\varepsilon_\omega^T\varepsilon_\omega/F_2) \varepsilon_\omega^T \dot{\varepsilon}_\omega \quad (25)$$

Considering the term expressed as follows, we have:

$$\begin{aligned}& k_2 \tanh(\varepsilon_\omega^T\varepsilon_\omega/F_2) \varepsilon_\omega^T \xi \mathbf{J}^{-1} \tilde{\mathbf{d}} \\ & \leq k_2 \tanh(\varepsilon_\omega^T\varepsilon_\omega/F_2) \frac{\lambda(\xi)_{\max}}{\lambda(\mathbf{J})_{\min}} D_m \left[|\varepsilon_{\omega i}| - \varepsilon_{\omega i} \tanh\left(\frac{\varepsilon_{\omega i}}{\mu_i}\right) \right] \\ & \leq k_2 \frac{\lambda(\xi)_{\max}}{\lambda(\mathbf{J})_{\min}} 0.2785 D_m \sum_{i=1}^3 \mu_i\end{aligned}\quad (26)$$

Substituting the actual control law into the equation (21) and combined with (25). Accordingly, define $\hat{D} = k_2 \frac{\lambda(\xi)_{\max}}{\lambda(\mathbf{J})_{\min}} 0.2785 D_m \sum_{i=1}^3 \mu_i$, $P = k_2 \tanh(\varepsilon_\omega^T\varepsilon_\omega/F_2)$, $R = \tanh\left(\frac{\varepsilon_q^T\varepsilon_q}{F_1}\right) \varepsilon_q^T \psi \mathbf{F}_e z_2$ the equation can be rearranged as:

$$\begin{aligned}\dot{V}_2 & \leq -K_\omega P \|\varepsilon_\omega\|^2 + K_u P \left(\frac{\|\varepsilon_\omega\|^2}{2} + \frac{\|\theta\|^2}{2} \right) \\ & \quad + P \left(\frac{\|\varepsilon_\omega\|^2}{2} + \frac{\|\xi\mathbf{J}^{-1}\Delta\tau\|^2}{2} \right) - R + \hat{D}\end{aligned}\quad (27)$$

In view of the fact in property (2), it should be noted that $PF_2 \left[\frac{\|\varepsilon_\omega\|^2}{F_2} \right] \geq k_2 F_2 \ln[\cosh(\varepsilon_\omega^T\varepsilon_\omega/F_2)] = 2V_2 \geq \frac{1}{2}PF_2 \left[\frac{\|\varepsilon_\omega\|^2}{F_2} \right]$. Hence, the inequality can be rearranged into the following form:

$$\begin{aligned}\dot{V}_2 & \leq -2K_\omega V_2 + 2K_u V_2 + 2V_2 + \frac{K_u k_2}{2} \|\theta\|^2 \\ & \quad + \frac{k_2}{2} \|\xi\mathbf{J}^{-1}\Delta\tau\|^2 + \hat{D} - R\end{aligned}\quad (28)$$

Take the time-derivative of V_3 , one can be obtained that:

$$\dot{V}_3 \leq -\left(K_a - \frac{1}{2}\right) \|\theta\|^2 - \left(K_b - \frac{1}{2}\right) \|\xi\mathbf{J}^{-1}\Delta\tau\|^2 \quad (29)$$

Take the time-derivative of V_4 , one can be obtained that:

$$\begin{aligned}\dot{V}_4 & = -C_q \|\Delta\rho_q\|^2 - C_\omega \|\Delta\rho_\omega\|^2 \\ & \quad + C_\tau \Delta\rho_q^T \xi \mathbf{J}^{-1} \text{vec}(|\tanh\Delta\tau_i|) \\ & \quad + B_\tau \Delta\rho_\omega^T \xi \mathbf{J}^{-1} \text{vec}(|\tanh\Delta\tau_i|)\end{aligned}\quad (30)$$

Applying the Young's inequality, the equation (30) can be further written as:

$$\begin{aligned}\dot{V}_4 & \leq -\frac{1}{2}(2C_q - C_\tau) \|\Delta\rho_q\|^2 - \frac{1}{2}(2C_\omega - B_\tau) \|\Delta\rho_\omega\|^2 \\ & \quad + \frac{1}{2}[C_\tau + B_\tau] \|\xi\mathbf{J}^{-1}\Delta\tau\|^2\end{aligned}\quad (31)$$

Define a composite Lyapunov function as $V = V_1 + V_2 + V_3 + V_4$, take the time-derivative of V and sort out all these results, we have the following conclusion:

$$\dot{V} \leq -S_1 V_1 - S_2 V_2 - S_3 V_3 - S_4 V_4 + \hat{D} \quad (32)$$

where $S_1 = \|q_{e0}\|M_\omega - 4\left(\frac{|\dot{\rho}_i|}{\rho_i}\right)_{\max}$, $S_2 = 2K_\omega - 2K_u - 2$, $S_3 = 2K_a - 1 - K_u k_2$, $S_4 = \min(2C_q - C_\tau, 2C_\omega - B_\tau)$. The main principle of the parameter selecting is S_1, S_2, S_3, S_4 should be guaranteed to be positive. Further, $2K_b - 1 - k_2 - C_\tau - B_\tau < 0$ should also be guaranteed to be satisfied. In view of these principle, it derives the following result:

$$\dot{V} \leq -\min(S_1, S_2, S_3, S_4) V + \hat{D} \quad (33)$$

In view of the final result, the ultimately boundedness of the system is ensured, the system will finally converge to a residual set. The state trajectory of q_{ev} and z_2 will converge to the desired performance constraint region, and all these performance requirements will be able to be satisfied. Here we give main principles for the parameter selecting.

1. To ensure that z_1 is able to converge, it should be guaranteed that $\|q_{e0}\|M_\omega - 4\left(\frac{|\dot{\rho}_{qi}|}{\rho_{qi}}\right)_{\max} > 0$ is always hold.

Considering about this term expressed as $\frac{|\dot{\rho}_{qi}|}{\rho_{qi}}$. As we stated in Remark 1, $t_1 - t_2$ can be set close enough to 0 practically, this ensures that the ρ_{qi} can be approximately regarded as an exponential-decayed one for the whole convergence stage. Hence, $\left(\frac{|\dot{\rho}_{qi}|}{\rho_{qi}}\right)_{\max} \approx l$ is satisfied in this way. **2.** Considering the last term in the control law (22), a small enough positive constant σ can be added to the denominator as $k_2 \tanh(\varepsilon_q^T\varepsilon_q/F_2) + \sigma$ to avoid the potential singularity problem.

VI. NUMERICAL SIMULATION

In this section, an assumed attitude tracking task is established, with specific requirements and constraints are presented for this virtual space mission. Simulation results are illustrated as below for the validation of the proposed scheme. The spacecraft is assumed to be a rigid-body one, of which the inertial matrix expressed in the body-fixed frame is expressed as $\mathbf{J} = \text{diag}(2.8, 2.5, 1.9) Kg \cdot m^2$. The external disturbance is supposed to be a time-varying one expressed as follows:

$$\mathbf{d} = \begin{bmatrix} 1e - 4 \cdot [4 \sin(3\omega_p t) + 3 \cos(10\omega_p t) - 20] \\ 1e - 4 [-1.5 \sin(2\omega_p t) + 3 \cos(5\omega_p t) + 20] \\ 1e - 4 [3 \sin(10\omega_p t) - 8 \cos(4\omega_p t) + 20] \end{bmatrix} \quad (34)$$

where $\omega_p = 0.01$. Further, the desired attitude quaternion q_d and the desired attitude angular velocity ω_d is set as follows:

$$\begin{aligned}q_d(0) & = [0.2, -0.5, -0.5, -0.6782]^T \\ \omega_d(t) & = 0.5[\cos(t/30), \sin(t/20), -\cos(t/40)]^T\end{aligned}\quad (35)$$

The constraint for the attitude tracking task is state as follows.

Physical Constraints. Physical constraints for the attitude tracking is elaborated as follows: **1.** The maximum rotation speed should not exceed $3^\circ/s$. **2.** The maximum output on each axis is assumed to be symmetric such that $\tau_m = 0.05Nm$, while the minima of controller output is assumed to be $1e - 4Nm$.

Performance Requirements. Performance requirements of the assumed attitude tracking task is stated as follows: **1.** The tracking error should converge to no more than $(|q_{evi}|)_{\max} < 5e - 3$ in no more than $60s$. **2.** The terminal control error should satisfy $|q_{evi}|_{\max} < 5e - 4$, which is corresponding to 0.03° .

A. Normal Case Attitude Tracking Simulation

The initial condition of the spacecraft is randomly chosen as follows:

$$\begin{aligned} \mathbf{q}_s(0) &= [0.1554, 0.4271, 0.4792, 0.7509]^T \\ \boldsymbol{\omega}_s(0) &= [0, 0, 0]^T \end{aligned} \quad (36)$$

Considering the fact that the maxima of the desired tracking angular velocity is $0.5 \cdot \frac{\sqrt{3}}{3} / s$, we set $k = 3$, $M_\omega = 0.017 = 1 \cdot \frac{\pi}{180}$ for safety consideration in this section. It should be noticed that the given desired angular velocity should not exceed the expected rotation rates limitation. Further, according to the performance requirements, the nominal PPF for q_e layer is designed in Table [I]:

Initial Value of Exponential Function Part ρ_{e0}	1
Terminal Value of Exponential Function Part $\rho_{e\infty}$	$1e-4$
Coefficient of Exponential Function Part l	0.05
Convergence Time of the RPF t_2	60
Terminal Value of the RPF g_∞	$5e-3$

TABLE I: Coefficients for the designed RPF ρ_q

Accordingly, to guarantee that the z_2 subsystem is able to converge in a short time, the nominal PPF for z_2 layer is designed in Table [II]:

Initial Value of Exponential Function Part ρ_{e0}	0.08
Terminal Value of Exponential Function Part $\rho_{e\infty}$	$1e-6$
Coefficient of Exponential Function Part l	0.5
Convergence Time of the RPF t_2	40
Terminal Value of the RPF g_∞	$3e-5$

TABLE II: Coefficients for the designed RPF for ρ_ω

In Figure[2] and Figure [3], it can be observed that both q_{ev} and z_2 is able to rapidly converge to the constraint region, and the performance requirements are satisfied. The terminal control error is bounded by $1e - 4$ which indicates that the given performance requirements are satisfied. It can be observed in Figure [5] that the maxima of the spacecraft's rotation speed is $2.1deg/s$, which is below the given limitation $3^\circ/s$. Also, the actual angular velocity rapidly converges to the desired signals, which is illustrated in dotted lines. The simulation result indicates that all the physical limitations, performance constraint are satisfied simultaneously.

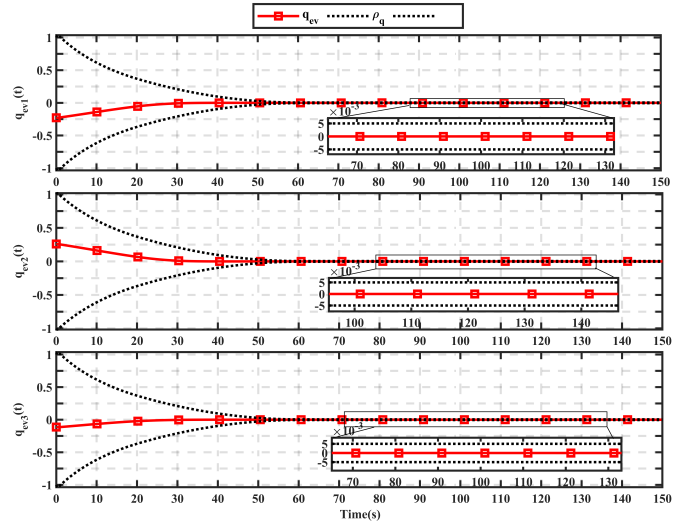


Fig. 2: Time Responding of q_{ev} (Normal Case)

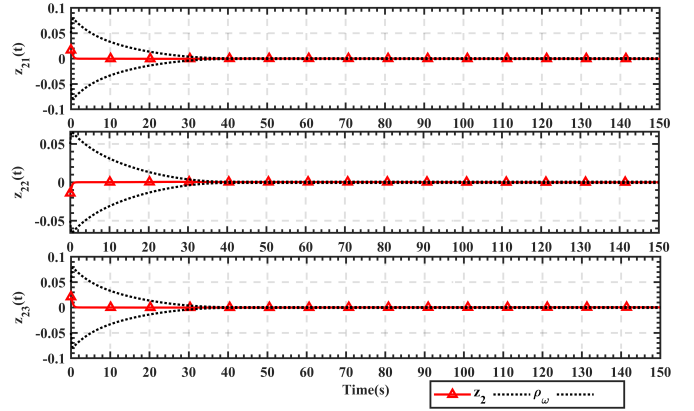


Fig. 3: Time Responding of z_2 (Normal Case)

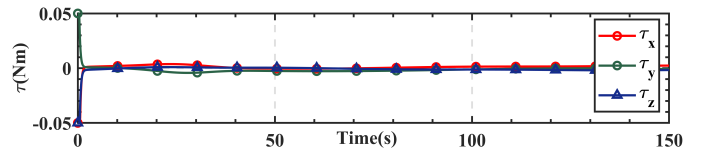


Fig. 4: Time Responding of τ (Normal Case)

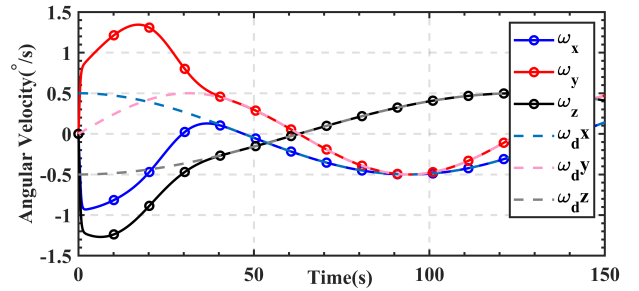


Fig. 5: Time Responding of ω_s (Normal Case)

B. Validation of Robustness

In this subsection, severe sudden disturbance will be exerted on the system in order to validate the robustness of the proposed scheme. An additional significant sudden external will be exerted to the system at $t = 20s$ and $t = 80s$. The proposed scheme is expected to re-stabilizing the spacecraft

in a short time after the sudden impact.

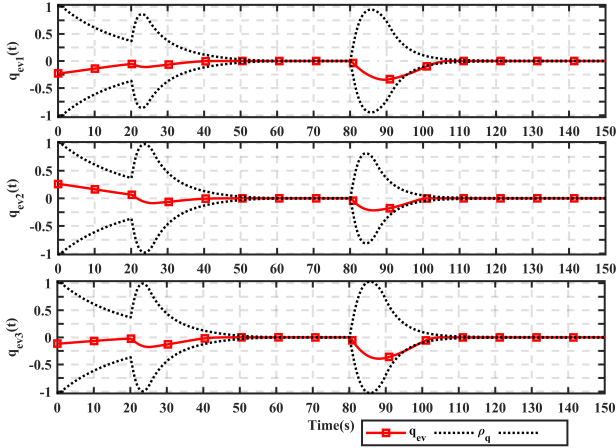


Fig. 6: Time Responding of q_{ev} (Sudden Disturbance Case)

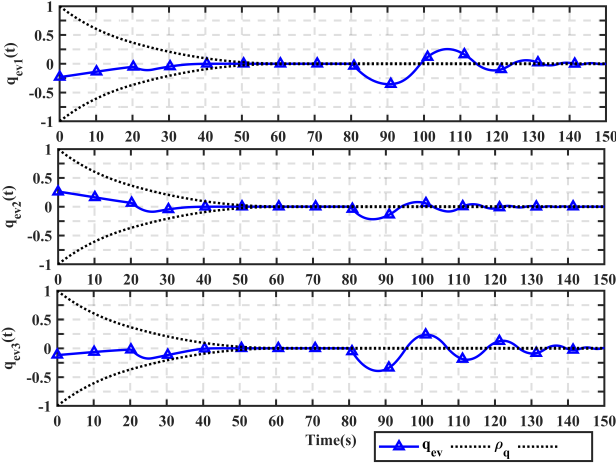


Fig. 7: Time Responding of q_{ev} Without Adaptive PPF (Sudden Disturbance Case)

The exerted sudden disturbance is modeled as follows: for $t = 20s$, $d_a = [0.5, 0.5, 0.5] N \cdot m$; for $t = 80s$, $d_a = [0.8, 0.8, 0.8] N \cdot m$. From Figure [6][8], it can be found that although the sudden severe disturbance critically perturbed the system, the proposed scheme is still able to recover in a short time. Also, the transient behavior of the re-stabilizing process is smooth and almost non-overshoot.

Here we make a simple comparison: we remove the adaptive strategy in the following simulation, which is illustrated in Figure[7][9]. It can be found that the recover time of the controller without adaptive PPF is much more longer than the other. Since the z_2 is the outer loop which is directly influenced by the disturbance, it can be observed that without the adaptive for PPF, the z_2 will chattering for a long time. This influences the tracking to the virtual control law, leading to the chattering of q_e finally.

C. Comparison to Traditional PPC

In this section, a BLF-based PPC benchmark controller is taken into considering to refer to as a comparison in the evaluation of the singularity circumvent effect. The benchmark

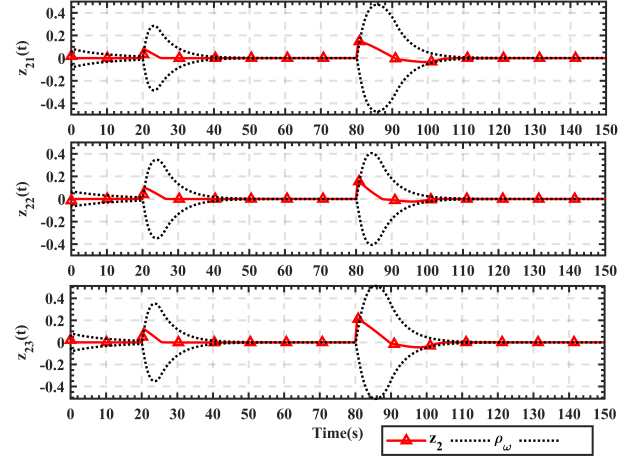


Fig. 8: Time Responding of z_2 (Sudden Disturbance Case)

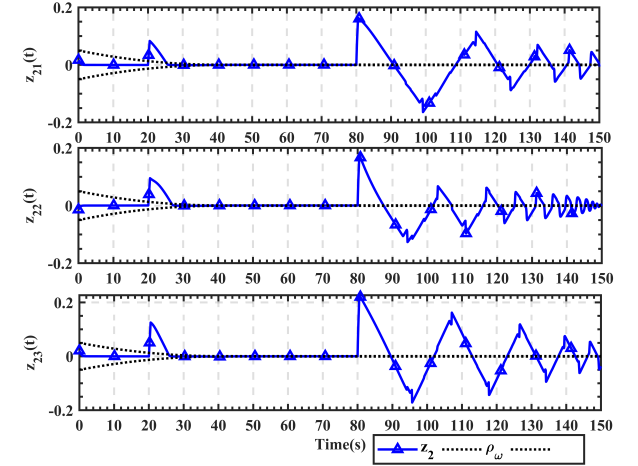


Fig. 9: Time Responding of z_2 Without Adaptive PPF (Sudden Disturbance Case)

controller is denoted as *TradBLF* in the subsection, and the detailed idea of the benchmark controller can be found in [18], which is designed based on a single-layer PPC structure. Here we omit it for brevity. In the comparison simulation, a sudden disturbances $d_a = [0.8; 0.8; 0.8]^T$ will be exerted to the system at $t = 80s$.

The simulation result of the benchmark controller and the proposed scheme is illustrated in Figure [10]. The blue line denotes the state trajectory of the benchmark controller, while the blue dotted line represents its corresponding PPF envelope. The state trajectory of the proposed scheme is illustrated in red line, while the red dotted line stands for its PPF.

When $t = 80s$, both two state trajectory is severely disturbed by the sudden disturbance, as we can find in Figure [10]. Notably, although the state trajectory of the benchmark controller is able to converge, it is failed to converge back to the constraint region. This phenomenon can be explained by the singularity of BLF-type PPC scheme, as we stated in [12]. The proposed scheme however, is able to stabilizing the system into the given region, guaranteeing the performance requirements to be satisfied. Further, the maximum angular velocity of *TradPPC* is much more bigger than the proposed

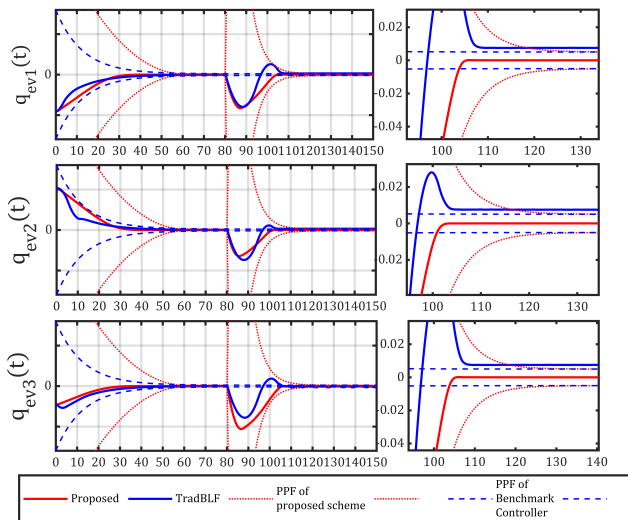


Fig. 10: Comparison of the proposed scheme and Benchmark Controller q_{ev}

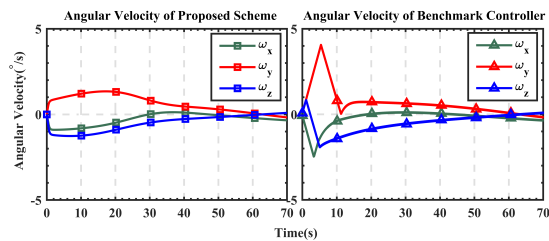


Fig. 11: Comparison of the proposed scheme and Benchmark Controller ω_s

scheme, as illustrated in Figure [11].

VII. CONCLUSION

This paper focuses on the space attitude tracking problem under physical limitations and performance requirements, with robustness in a critical position during the controller design. For the robustness issue, the inherent singularity problem is tackled by the newly-designed BLF. Owing to the proposed adaptive strategy for PPF, the chattering problem is significantly alleviated, which provides smooth convergence of the system after severe disturbances. Subsequently, the angular velocity constraint is satisfied by applying the proposed BLF, and the input saturation issue is solved by introducing the auxiliary system. Based on the designed BLF, we derive a backstepping controller with a double-layer PPC structure, ensuring that the performance requirements can be satisfied. The numerical simulation results validate our theoretical analysis, providing convincing support for the proposed scheme. Further research in this issue will focus on other more complex constraints, such as the pointing constraints, which are hard to fuse with the performance requirements up to now and worth further investigation.

REFERENCES

[1] B. Wie and J. Lu, "Feedback control logic for spacecraft eigenaxis rotations under slew rate and control constraints," *Journal of Guidance, Control, and Dynamics*, vol. 18, no. 6, pp. 1372–1379, 1995. [Online]. Available: <https://doi.org/10.2514/3.21555>

[2] Q. Hu, B. Li, and Y. Zhang, "Robust attitude control design for spacecraft under assigned velocity and control constraints," *ISA transactions*, vol. 52, no. 4, pp. 480–493, 2013. [Online]. Available: <https://doi.org/10.1016/j.isatra.2013.03.003>

[3] M. Li, M. Hou, and C. Yin, "Adaptive attitude stabilization control design for spacecraft under physical limitations," *Journal of guidance, control, and dynamics*, vol. 39, no. 9, pp. 2179–2183, 2016. [Online]. Available: <https://doi.org/10.2514/1.G000348>

[4] X. Shao, Q. Hu, Y. Shi, and B. Jiang, "Fault-tolerant prescribed performance attitude tracking control for spacecraft under input saturation," *IEEE Transactions on Control Systems Technology*, vol. 28, no. 2, pp. 574–582, 2018. [Online]. Available: <https://doi.org/10.1109/TCST.2018.2875426>

[5] L. Sun and Z. Zheng, "Disturbance-observer-based robust backstepping attitude stabilization of spacecraft under input saturation and measurement uncertainty," *IEEE Transactions on Industrial Electronics*, vol. 64, no. 10, pp. 7994–8002, 2017. [Online]. Available: <https://doi.org/10.1109/TIE.2017.2694349>

[6] A.-M. Zou, A. H. de Ruiter, and K. D. Kumar, "Finite-time output feedback attitude control for rigid spacecraft under control input saturation," *Journal of the Franklin Institute*, vol. 353, no. 17, pp. 4442–4470, 2016. [Online]. Available: <https://doi.org/10.1016/j.jfranklin.2016.08.013>

[7] Q. Hu, Y. Shi, and X. Shao, "Adaptive fault-tolerant attitude control for satellite reorientation under input saturation," *Aerospace Science and Technology*, vol. 78, pp. 171–182, 2018. [Online]. Available: <https://doi.org/10.1016/j.ast.2018.04.015>

[8] C. Zhang, G. Ma, Y. Sun, and C. Li, "Observer-based prescribed performance attitude control for flexible spacecraft with actuator saturation," *ISA transactions*, vol. 89, pp. 84–95, 2019. [Online]. Available: <https://doi.org/10.1016/j.isatra.2018.12.027>

[9] C. Wei, J. Luo, H. Dai, and G. Duan, "Learning-based adaptive attitude control of spacecraft formation with guaranteed prescribed performance," *IEEE transactions on cybernetics*, vol. 49, no. 11, pp. 4004–4016, 2018. [Online]. Available: <https://doi.org/10.1109/TCYB.2018.2857400>

[10] C. Wei, Q. Chen, J. Liu, Z. Yin, and J. Luo, "An overview of prescribed performance control and its application to spacecraft attitude system," *Proceedings of the Institution of Mechanical Engineers, Part I: Journal of Systems and Control Engineering*, vol. 235, no. 4, pp. 435–447, 2021. [Online]. Available: <https://doi.org/10.1177/0959651820952552>

[11] C. P. Bechlioulis and G. A. Rovithakis, "Adaptive control with guaranteed transient and steady state tracking error bounds for strict feedback systems," *Automatica*, vol. 45, no. 2, pp. 532–538, 2009. [Online]. Available: <https://doi.org/10.1016/j.automatica.2008.08.012>

[12] J. Lei, T. Meng, W. Wang, H. Li, and Z. Jin, "Singularity-avoidance prescribed performance attitude tracking of spacecraft," 2022. [Online]. Available: <https://doi.org/10.48550/arXiv.2206.12761>

[13] K. Yong, M. Chen, Y. Shi, and Q. Wu, "Flexible performance-based robust control for a class of nonlinear systems with input saturation," *Automatica*, vol. 122, 2020. [Online]. Available: <https://doi.org/10.1016/j.automatica.2020.109268>

[14] K. Wang, T. Meng, W. Wang, R. Song, and Z. Jin, "Finite-time extended state observer based prescribed performance fault tolerance control for spacecraft proximity operations," *Advances In Space Research*, 2022. [Online]. Available: <https://doi.org/10.1016/j.asr.2022.05.072>

[15] M. Golestani, S. Mobayen, S. U. Din, F. F. El-Sousy, M. T. Vu, and W. Assawinchaichote, "Prescribed performance attitude stabilization of a rigid body under physical limitations," *IEEE Transactions on Aerospace and Electronic Systems*, 2022. [Online]. Available: <https://doi.org/10.1109/TAES.2022.3158371>

[16] B. Xiao, Q. Hu, and Y. Zhang, "Adaptive sliding mode fault tolerant attitude tracking control for flexible spacecraft under actuator saturation," *IEEE Transactions on Control Systems Technology*, vol. 20, no. 6, pp. 1605–1612, 2011. [Online]. Available: <https://doi.org/10.1109/TCST.2011.2169796>

[17] C. P. Bechlioulis and G. A. Rovithakis, "Robust adaptive control of feedback linearizable mimo nonlinear systems with prescribed performance," *IEEE Transactions on Automatic Control*, vol. 53, no. 9, pp. 2090–2099, 2008. [Online]. Available: <https://doi.org/10.1109/TAC.2008.929402>

[18] Q. Hu, Y. Shi, and X. Shao, "Adaptive fault-tolerant attitude control for satellite reorientation under input saturation," *Aerospace Science and Technology*, vol. 78, pp. 171–182, 2018. [Online]. Available: <https://doi.org/10.1016/j.ast.2018.04.015>